Order, Disorder, and Composition Fluctuation Effects in Low Molar Mass Hydrocarbon−Poly(dimethylsiloxane) Diblock Copolymers

Kristoffer Almdal* and Kell Mortensen

Department of Solid State Physics, Risø National Laboratory, P.O Box 49, DK-4000 Roskilde, Denmark

Anthony J. Ryan

Manchester Materials Science Centre, UMIST, Grosvenor Street, Manchester M1 7HS, U.K., and CCLRC Daresbury Laboratory, Warrington, WA4 4AD, U.K.

Frank S. Bates

Department of Chemical Engineering and Materials Science, University of Minnesota, Minneapolis, Minnesota 55405-0132

Received March 21, 1996; Revised Manuscript Received June 10, 1996[⊗]

ABSTRACT: Four block copolymer melts—two poly(isoprene-*block*-dimethylsiloxane) (PI−PDMS) and two poly(ethylene-*alt*-propylene-*block*-dimethylsiloxane) (PEP−PDMS)—have been investigated through rheological measurements, SANS, and SAXS. In both systems, lamellar to disorder and $Ia\bar{3}d$ bicontinuous to disorder transitions have been observed. Upon heating, the sequence of phases lamellae, modified layers, bicontinuous $Ia\bar{3}d$, disorder is observed in the $f = 0.65$ PEP−PDMS sample. Composition fluctuations dominate the disordered state properties over an unprecedented wide temperature window in the $f = 0.49$ PEP−PDMS sample. The fluctuations are evident both in SANS measurements and through the temperature dependence of the viscosity. The phase behavior of these relatively low molar mass block copolymer melts, which range from 6 to 10 kg/mol, is qualitatively anticipated by the trends reported earlier for progressively lower molar mass diblock copolymers.

1. Introduction

Block copolymer melts exhibit behavior remarkably similar to conventional amphiphilic systems such as lipid−water mixtures, soap, and surfactant solutions. The incompatibility between the blocks leads at sufficiently high molar masses to the formation of ordered structures. The connectivity between chemically distinct blocks imposes severe constraints on the possible equilibrium states: microdomain structures such as lamellae (LAM), hexagonally packed rods (HEX), and spheres packed on a body-centered cubic lattice (BCC) are restricted to form with lattice parameters of the order of the radius of gyration of the chains ($R_g = b(N/6)^{1/2}$, where b is the statistical segment length, and N the overall degree of polymerization). Consequently, the Fourier transform of the two-point correlation function, $S(\mathbf{q})$, shows a pronounced peak at $q^* = |\mathbf{q}^*| \sim R_g^{-1}$. Theories of AB diblock copolymer phase behavior are usually cast in terms of two parameters, f, the volume fraction of block A, and the product χN, where χ is the Flory−Huggins interaction parameter. Differences in block conformations are easily accounted for by a third parameter, $\epsilon = (R_{g,A}/R_{g,B})^2(V_B/V_A)$, where V is the volume of the polymer.[1−3] In both the strong segregation and weak segregation limit (SSL and WSL, respectively), the behavior of block copolymer melts can be reasonably well described in a mean-field approximation.[4−6]

In the intermediate regime, around $\chi N \simeq 10$, where the transition from a spatially homogeneous (disordered) state to a microphase-separated (ordered) state occurs, the mean-field picture must be corrected for fluctuation effects. Fredrickson and Helfand[7] extended Leibler's mean-field treatment of block copolymer melts in the WSL approximation[4] to include composition fluctuations. The fluctuation effect produces an $O(\bar{N}^{-1/3})$ correction to the mean-field order to disorder transition (ODT) prediction, where $\bar{N} = R_g^6/V^2 = Nb^6v^{-2}$, and v is the volume of the statistical segment. The fluctuation picture of the disordered state as described by Fredrickson and Helfand has in many respects been experimentally confirmed.[8,9] The temperature dependence of the inverse scattering intensity at q^*, $I^{-1}(q^*)$, of a variety of nearly symmetric ($f = 0.55 \pm 0.05$) diblock copolymers has been found to be a nonlinear function of the inverse absolute temperature, T^{-1}, in close agreement with the theory. However, it was also shown that the mean-field structure factor, $S(q)$, does not quantitatively account for the experimental structure factor in the vicinity of the ODT.

In a previous study, the $\bar{N}$ dependence of block copolymer melt phase behavior in the ordered state close to the ODT ($\chi N \gtrsim 10$) was investigated.[2] Investigating the effect of varying chain length on phase behavior while keeping χN approximately constant can only be accomplished by looking at a wide variety of chemically different block copolymer systems. In the poly(ethylene)-*block*-poly(ethylenepropylene) (PE−PEP) system, a block copolymer characterized by $f = 0.5$ has an order−disorder transition (ODT) at 150 °C when $M_n = 1.18 \times 10^5$ g/mol ($\bar{N} = 2.7 \times 10^4$). In poly(isoprene-*block*-styrene) (PI−PS), the ODT is obtained at the same temperature with $M = 1.8 \times 10^4$ g/mol ($\bar{N} = 1.1 \times 10^3$). We have shown that the composition window for the different ordered states depends on both the conformational asymmetry and $\bar{N}$. Most striking is the absence of the bicontinuous phase at high $\bar{N}$ and the increasingly larger sizes of the stability windows for this phase in f versus (χN) diagrams as $\bar{N}$ decreases. This and other

* To whom correspondence should be addressed.
[⊗] Abstract published in *Advance ACS Abstracts,* August 1, 1996.

S0024-9297(96)00437-8 CCC: $12.00

Scheme 1

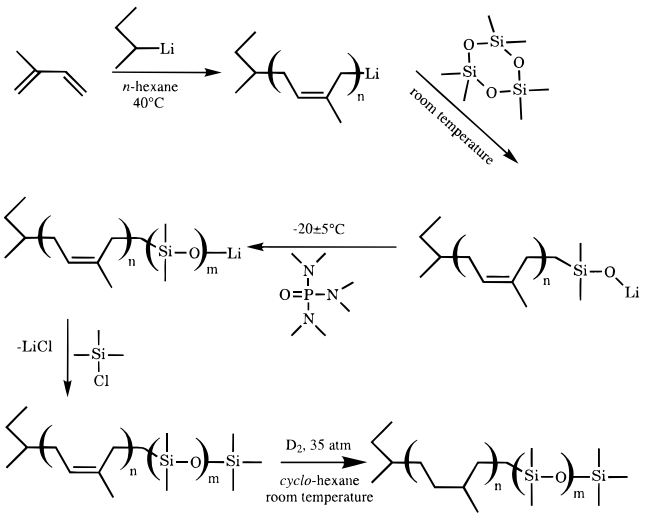

complex phases appear to be stabilized by intermediate chain lengths where the chains are long enough to possess the flexibility needed to form curved interfaces yet short enough to produce packing frustration that destabilizes the HEX[1] and LAM phases.

We suspect that in the limit of very short diblocks which are characterized by very large incompatibilities between the blocks, this trend will break down. In that limit, the molecules would behave more like rigid rods rather than flexible chains. Rigid rods are well established to from nematic and smectic phases.[10] Thus, we expect that as the block copolymer molar mass is progressively reduced, while maintaining $\chi N \sim 10$, the stability window of the LAM phase will increase and eventually the complex mono- and bicontinuous phases will be squeezed out.

These considerations have prompted us to search for new block copolymer systems with strong repulsive interactions between the two blocks in order to be able to study the phase behavior close to the ODT in small (polymeric) molecules. Obvious candidates for such systems are poly(dimethylsiloxane) (PDMS) and poly(ethylene oxide) (PEO) containing block copolymers. In this paper, we report our first findings for the systems poly(isoprene-*block*-dimethylsiloxane) (PI−PDMS) and poly(ethylene-*alt*-propylene-*block*-dimethylsiloxane) (PEP−PDMS). We have focused our attention on two particular compositions, close to $f = 0.5$ and close to $f = 0.65$, where LAM and bicontinuous cubic ordered phases, have been observed in other block copolymer systems. Low molar mass PEO-based block copolymer melts are described in a separate publication.[11]

2. Experimental Section

The synthesis of the PDMS-containing copolymers has necessitated a study of the polymerization of hexamethylcyclotrisiloxane (D_3) in hydrocarbon solvents with lithium as the counterion. The use of a hydrocarbon solvent is necessary in order to obtain the desired microstructure in the hydrocarbon part of the block copolymers. The synthesis procedure is outlined in Scheme 1. Details of this study will be presented elsewhere.[12]

Two poly(isoprene)−poly(dimethylsiloxane) (PI−PDMS) diblock copolymers were synthesized by anionic polymerization of isoprene in *n*-hexane at 40 °C using *sec*-butyllithium as initiator followed by addition of D_3, cooling to approximately −20 °C, addition of hexamethylphosphoric triamide (HMPA), and termination by addition of a 1.5-fold excess of trimethylchlorosilane. The resulting PI−PDMS block copolymers were saturated with deuterium at 35 atm using palladium (5%) on calcium carbonate as catalyst. Note that the procedure yields pairs of PI−PDMS and PEP−PDMS with the same number of atoms in the main chain. The molecular details of the materials described in this work are given in Table 1.

Table 1

sample	$M_n{}^a$/(kg/mol)	$M_n{}^b$/(kg/mol)	$f^{a,c}$	$f^{b,c}$	$N^{c,d}$	$\bar{N}^d$
PI−PDMS-6	6.3 ± 0.1	6.2	0.47	0.46	102	257
PEP−PDMS-6	6.4 ± 0.1	6.3	0.49	0.48	106	384
PI−PDMS-7	10.5 ± 0.2	10.2	0.64	0.63	175	490
PEP−PDMS-7	10.7 ± 0.2	10.4	0.65	0.65	183	800

[a] Calculated from stoichiometry. [b] From NMR. [c] Assuming no volume change on mixing, $\rho_{PI}/\rho_{PDMS} = 0.9260$, $\rho_{PEP}/\rho_{PDMS} = 0.8852$, and $\rho_{PDMS} = 970$ kg/m^3. [d] At 150 °C; $\nu/m^3 = 8.8 \times 10^{-29} \exp[6.85 \times 10^{-4}(T/K)]$; $a^2_{X-PDMS} = f a^2_X + (1 - f) a^2_{PDMS}$, where X is PI or PEP; $a_{PI}(150°) = 6.055$ Å; $a_{PEP} = 8.6 \exp[-5.8 \times 10^{-4}(T/K)]$; $a_{PDMS} = 4.65 \exp[3.5 \times 10^{-4}(T/K)]$.

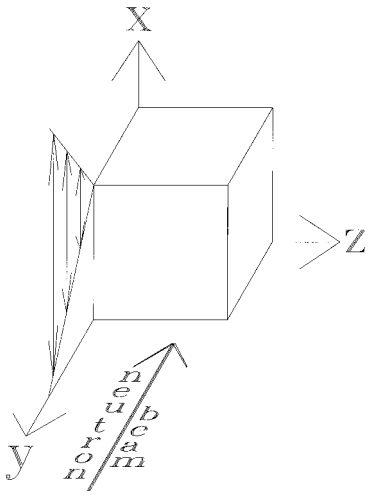

Figure 1. Geometry of the neutron beam and the shearing device. Scattering patterns for other directions than the shear gradient direction, **y**, are obtained by turning either small pieces of sample or the whole cell in the beam.

Dynamical mechanical measurements in the shear sandwich geometry were conducted using a Rheometrics RSA2 solids analyzer. Dynamical mechanical measurements and viscosity measurements in the cone-and-plate geometry were conducted with a Rheometrics RMS800 mechanical spectrometer. During the measurements, the samples were kept in a temperature-controlled nitrogen atmosphere.

Small-angle neutron scattering (SANS) experiments were conducted at the 12 m SANS facility at Risø National Laboratory, Denmark, using 5.54 Å wavelength neutrons with a wavelength distribution $\Delta\lambda/\lambda = 0.09$. Scattered neutrons were detected on a circular area detector. The reported intensities were corrected for background and are given in arbitrary units. For experiments in shear fields, the samples were placed between two 25.4 mm × 25.4 mm aluminum plates. The sample thickness was controlled by milled groves in the aluminum plates.[13] The samples were mounted in a device designed to subject the samples to reciprocating simple shear while being studied in the neutron beam.[14] The geometry of the experiment (with reference to Figure 1) is such that the sample is sheared in the **x** direction, while the shear gradient is in the **y** direction and the neutron beam is in the **y** direction. The amplitude of the triangular wave that describes the sample deformation is adjustable. For experiments under static, *i.e.*, zero shear field, conditions, the samples were placed in 1 mm path length quartz cuvettes and thermostated in a specially designed set of brass blocks held in the sample position of the shearing device.

Small-angle X-ray scattering (SAXS) experiments were conducted on beam line 8.2 at the CCLRC Daresbury Synchrotron Radiation Source. Details of the storage ring, radiation (λ = 1.5 Å), camera geometry, and data collection

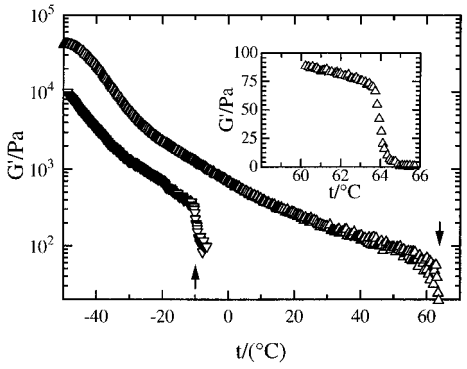

Figure 2. Dynamical mechanical elastic moduli as a function of temperature for samples PI−PDMS-6 (▽) and PEP−PDMS-6 (△). All data were measured with $\omega = 10$ rad/s; strain amplitude, $\gamma_0 = 5\%$ in a shear sandwich geometry. Heating rate: 1 °C/min (▽), 2 °C/min (△). T_{ODT}'s are indicated with arrows. The inset shows the dynamical mechanical elastic moduli as a function of temperature for sample PEP−PDMS-6 measured in a cone-and-plate geometry ($\omega = 10$ rad/s, strain amplitude of 5%, heating rate 0.1 °C/min).

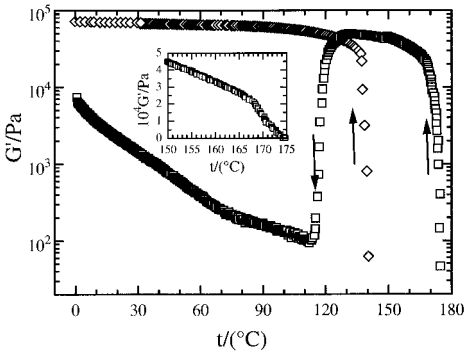

Figure 3. Dynamical mechanical elastic moduli as a function of temperature for samples PI−PDMS-7 (◇) and PEP−PDMS-7 (□). $\omega = 10$ rad/s; $\gamma_0 = 5\%$; shear sandwich geometry. T_{ODT}'s and T_{OOT} are indicated with arrows. Heating rate: 5 °C/min (◇), 1 °C/min below 150 °C and 0.5 °C/min above 150 °C (□). The inset shows data for PEP−PDMS-7 close to the ODT plotted on a linear scale; $\omega = 10$ rad/s, $\gamma_0 = 5\%$.

electronics have been given elsewhere.[15] The camera was equipped with a multiwire quadrant detector located 3.5 m from the sample position. The sample was mounted in a DSC pan (fitted with Mica windows (7 mm diameter) and a 0.7 mm spacer) or a Linkarn microscope hot stage. Data was corrected for transmission and detector linearity. No background was subtracted as the scattered intensity was 3 orders of magnitude stronger than that of the empty cell.

3. Results and Analysis

3.1. Phase Transitions. The temperatures at which order to disorder (T_{ODT}) and order to order (T_{OOT}) transitions occur were probed by dynamical mechanical measurements.[16,17]

In Figures 2 and 3, the results of such experiments for the four samples listed in Table 1 are given. The data in Figure 2 show T_{ODT}'s at −10 and +64 °C for samples PI−PDMS-6 and PEP−PDMS-6, respectively. For low values of G', *i.e.*, below 200 Pa, the data obtained using the shear sandwich geometry are noisy due to a lack of sensitivity. However, data obtained using the cone-and-plate geometry (inset in Figure 2) show that the ODT for sample PEP-PDMS-6 is a sharp transition that occurs within the temperature resolution of the instrument (0.5 °C). Thus the data indicate one ordered phase below T_{ODT} and disorder above T_{ODT} for both PI−PDMS-6 and PEP−PDMS-6.

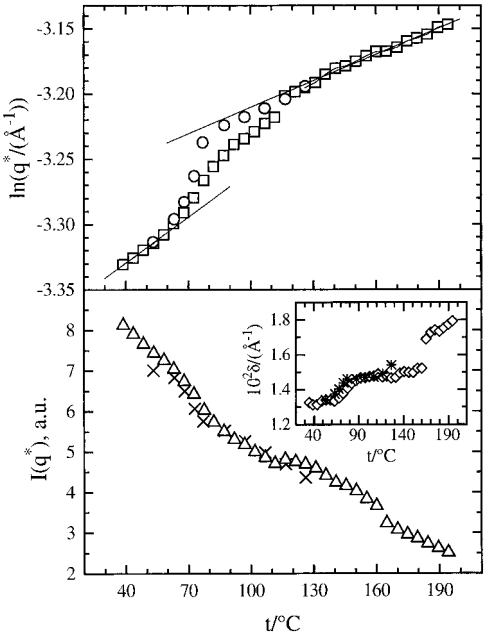

Figure 4. SANS data for sample PEP−PDMS-7 plotted as a function of temperature. A Gaussian function was fit to the azimuthally averaged data to obtain q^*, $I(q^*)$, and δ. The errors in the fit are approximately the size of the points ($I(q^*)$, δ) or smaller (q^*). Upper: ln q^*, increasing temperature (□); decreasing temperature (○). The lines are added to guide the eye. Lower: $I(q^*)$, increasing temperature (△); decreasing temperature (×). Inset: δ, increasing temperature (◇); decreasing temperature (*).

The data in Figure 3 show T_{ODT}'s at (135 ± 2) and (170 ± 4) °C for samples PI−PDMS-7 and PEP−PDMS-7, respectively. However, it is clear from the inset in Figure 3, where the PEP−PDMS-7 data close to T_{ODT} we reproduced on a linear scale, that there is no clear discontinuity in $G'(T)$ but only a change in the form of the curve. This is also the case for PI−PDMS-7 (not shown). Note that SANS data indicate a lower T_{ODT}; see below. This is most likely due to a complex frequency dependence of G' and G'' for the bicontinuous phase near the ODT as discussed in a separate publication.[18]

Figure 3 also indicates at least one transition between two ordered states at $T_{OOT} = 115$ °C. The change in slope at approximately 80 °C may also represent a phase transition. This feature is more convincingly examined with SANS data. Another noticeable feature of Figure 3 is the very high and nearly identical elastic moduli characterizing the ordered phases in the two samples just below T_{ODT}. The plateau moduli at 25 °C of PEP and PDMS are $G^{\circ}_{N,PEP} = 1.15$ MPa[19,20] and $G^{\circ}_{N,PDMS} = 0.20-0.24$ MPa,[19,20] respectively.

SANS data were obtained from a macroscopically isotropic sample of PEP−PDMS-7, *i.e.*, a sample that was heated above T_{ODT} and quenched to room temperature before the measurement. The data were azimuthally averaged and a Gaussian function was fit to the data at each temperature to obtain the peak position, q^*, the peak intensity, $I(q^*)$, and the peak width at half-maximum, δ. These fitted parameters are presented in Figure 4. Several features are noticeable. On heating, two deviations from the linear increase in ln q^* due to coil contraction are observed. Between 70 and 90 °C, a continuous increase occurs, and at 115 °C a small but distinct discontinuous jump is observed. On cooling, no discontinuity at 115 °C is observed. However, a relatively sharp continuous change around 70 °C brings the

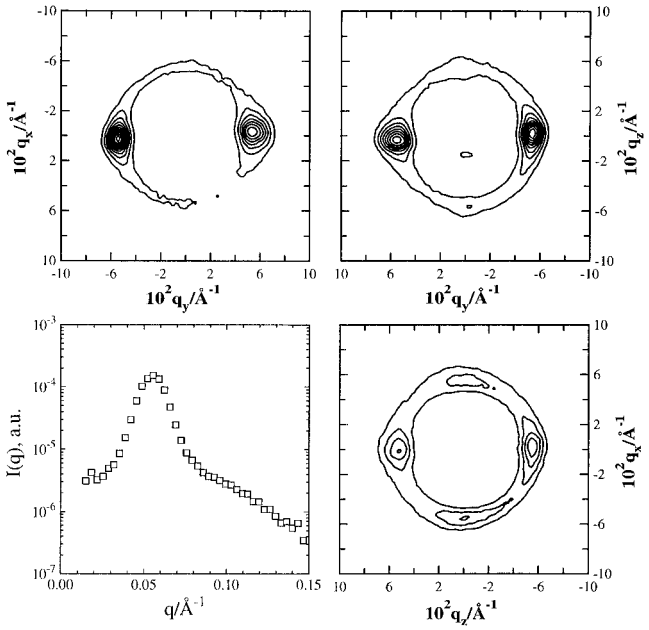

Figure 5. SANS data for sample PEP−PDMS-6. A piece of sample (approximately 2 × 2 × 0.5 mm^3) was sheared at room temperature by manually sliding the two aluminum plates back and forth with an amplitude of approximately 2 mm and a frequency of order 1 Hz for 1 min. Scattering from this sample collected in the three principal directions, **x**, **y**, and **z**, is shown in the upper right, the lower right, and the upper left corners, respectively, in accordance with the convention outlined in Figure 1. Equidistant contours on a linear scale are drawn. Scattering from a macroscopically isotropic sample at 34 °C is shown in the lower left corner.

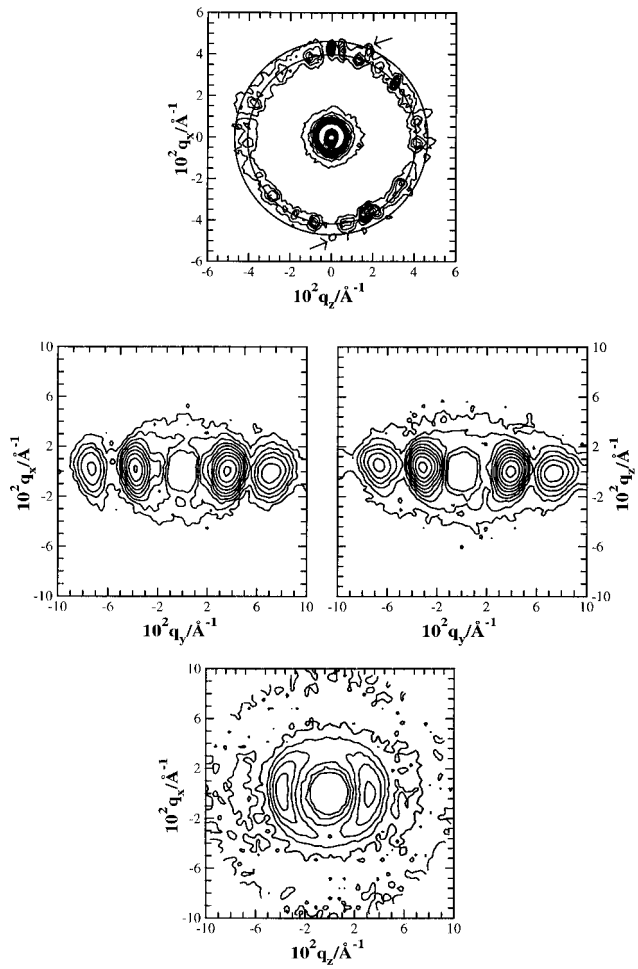

Figure 6. SANS patterns from sample PEP−PDMS-7. In a 1.2 mm thickness shear cell, the sample was sheared at room temperature by manually sliding the two aluminum plates back and forth with a strain amplitude of approximately 200% for 50 cycles at a frequency of order 1 Hz. Bottom pattern: at 25 °C; four equidistant contours per decade on a log scale are drawn. Central patterns: Subsequently the cell was quenched in liquid nitrogen and the cell opened. Small pieces of sample (approximately 2 × 2 × 1.2 mm^3) were cut out and placed in the beam exposing the **x** and **z** directions, respectively. During this procedure, the sample was kept chilled with liquid nitrogen. Four equidistant contours per decade on a log scale are drawn. Top pattern: A 0.2 mm thick sheared sample (60 °C, 350% strain amplitude, and $\dot{\gamma} = 5.6$ s^{-1}) was heated to 120 °C. The inner circle in this pattern represents q^*. The outer circle is generated such that the ratio of q values on the two circles is $(4/3)^{1/2}$. Two of several (220) reflections are indicated with arrows. Equidistant contours on a linear scale are drawn.

value of ln q^* back to where it started close to room temperature. Thus between 80 and 115 °C a state is accessed upon heating that appears to be bypassed on cooling. Above 120 °C complete reversibility is observed. Heating and cooling through the ODT produces no noticeable change in ln q^*. In $I(q^*)$ changes occur at 70−90 °C, at 115 °C, and most noticeable a discontinuity at (160 ± 2) °C that signals the ODT. In δ a big discontinuous jump is observed at (160 ± 2) °C and a continuous change occurs between 70 and 90 °C.

Thus, in conclusion, the macroscopically isotropic SANS and rheology data for sample PEP−PDMS−7 indicate four phases: an ordered phase below 70 °C that is accessed on cooling slowly or quenching quickly from disorder; an ordered phase between 70 and 115 °C that can only be accessed by heating from the low-temperature phase (this is not necessarily an equilibrium phase); an ordered phase between 115 and 160 °C (this phase is stable down to approximately 90 °C on cooling); and finally the disordered phase above 170 °C. For sample PI−PDMS-7, one ordered phase below T_{ODT} and disorder above T_{ODT} are indicated.

3.2. Ordered State Structure. In order to elucidate the structure of the samples in the ordered state, SANS patterns were recorded from samples that had been subjected to large-strain amplitude oscillatory shear. This technique often places ordered block copolymer specimens in a "single crystal" or at least partially oriented form, thereby facilitating the assignment of ordered state symmetry.[17,21−23]

In the case of sample PEP−PDMS-6, it was not possible to cut small pieces of shear-oriented material at room temperature due to the combined effect of low molar mass and low glass transition temperatures of PEP and PDMS. Instead a small specimen approximately 2 × 2 × 0.5 mm^3 was sheared in a custom-made aluminum holder which was mounted in the beam at different orientations. In Figure 5, two-dimensional SANS patterns obtained from this sample are shown. Although the orientation is far from perfect, distinct characteristics appear from the three orientations. The anisotropy in the scattering in the (q_x,q_z) plane is weak whereas the data in the two other orientations are consistent with LAM aligned with the layers perpendicular to the **y** direction, *i.e.*, parallel lamellae. Additional evidence for the LAM structure comes from the isotropic SANS pattern from sample PEP−PDMS-6 (Figure 5), which shows a broad and weak but distinct second-order reflection at $q = 2q^*$. Thus, we conclude that sample PEP−PDMS-6 is LAM in the ordered state. Based on the analogy of the rheology traces between samples PI−PDMS-6 and PEP−PDMS-6, we believe

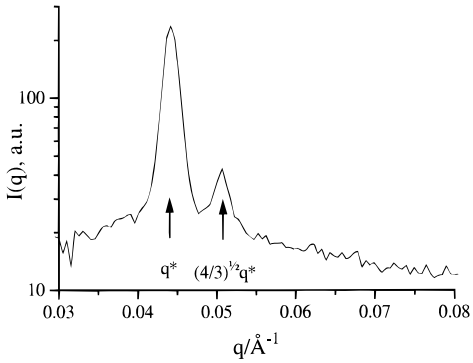

Figure 7. Azimuthally averaged small-angle X-ray scattering data for sample PI−PDMS-7. The arrows indicate the relative position of the first two characteristic reflections, (211) and (220), of the $Ia\bar{3}d$ structure.

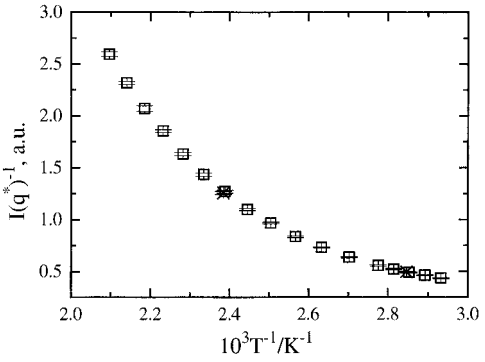

Figure 8. SANS data for sample PEP−PDMS-6 plotted as a function of inverse temperature: increasing temperature (□); decreasing temperature (×).

PI−PDMS-6 is also LAM in the ordered state. The phase state in the PI−PDMS system is not easy to evaluate due to insignificant SANS contrast and weak X-ray contrast.

Scattering from the low-temperature ordered phase in sample PEP−PDMS-7 is given in the lower three panels of Figure 6. In this case, it was feasible to shear and cut pieces of sample at low temperature, *i.e.*, below T_g of PEP. All three principal directions show anisotropic scattering patterns. However, the anisotropy in the (q_x,q_z) plane is weak, whereas both the (q_x,q_y) plane and the (q_y,q_z) plane show strong anisotropy. In all three directions, higher order reflections at $q = 2q^*$ are seen. This structure is interpreted to be LAM preferentially oriented with the layers perpendicular to the **y** direction with some minor amount of misaligned or deformed material.

When an oriented PEP−PDMS-7 was heated, the anisotropy was maintained but the weak higher order reflections evident in the (q_y,q_z) plane were lost between 80 and 110 °C (not shown). Based on a persistent anisotropy and low overall intensity, we have concluded that this intermediate state is still layered, possibly hexagonally perforated layers (HPL) or hexagonally modulated lamellae (HML).[24] The structure of this phase and the transition between this phase and the high-temperature ordered phase in PEP−PDMS-7 will be the subject of a separate publication.[25]

When a similarly oriented PEP−PDMS-7 sample was heated to 120 °C, the scattering changed dramatically (top panel, Figure 6). Well-defined Bragg reflections indicate a highly textured piece of material. By configuring the SANS instrument at the highest possible resolution, two tightly spaced sets of reflections could be resolved. The ratio of the associated q values is consistent with $(4/3)^{1/2}$, which is expected from the first two, *i.e*, (211) and (220), reflections from structures belonging to the cubic $Ia\bar{3}d$ space group symmetry. Ordered cubic structures have been shown to have high moduli.[14,26] Thus the SANS data combined with the high G' for the high-temperature ordered state in PEP−PDMS-7 lead us to conclude that this phase has the $Ia\bar{3}d$ structure, which is the same bicontinuous morphology recently identified in other diblock copolymers near the ODT.[26,27]

In Figure 7, synchrotron X-ray data for sample PI−PDMS-7 are presented. As with the high-temperature ordered phase in PEP−PDMS-7, two well-resolved reflections are observed consistent the $Ia\bar{3}d$ structure. Note that the elastic moduli of the $Ia\bar{3}d$ structure in PI−PDMS-7 and PEP−PDMS-7 are closely matched.

Thus, we conclude that sample PI−PDMS-7 is the ordered bicontinuous $Ia\bar{3}d$ morphology below T_{ODT} and disordered above T_{ODT}. Sample PEP−PDMS-7 is ordered LAM below approximately 80 °C, a modified layered structure between 80 and 115 °C, bicontinuous $Ia\bar{3}d$ between 115 °C and T_{ODT}, and disordered above T_{ODT}. The modified layered structure that occurs between the LAM and $Ia\bar{3}d$ morphologies is only accessed upon heating and may thus be a metastable phase.

3.3. The Disordered State. SANS data were measured from an isotropic sample of PEP−PDMS-6 between room temperature and 204 °C. The data were azimuthally averaged and a Lorentzian function, $I(q) = I(q^*)/(1 + (q - q^*)^2\xi^2)$, corrected for instrumental smearing,[28] was fit over a narrow q range around q^* at each temperature to obtain the peak position, q^*, the peak intensity, $I(q^*)$, and the correlation length, ξ. The fitted parameters are presented in Figures 8 and 9. The lack of absolute intensity data complicates a fit of the disordered state data to the structure factor commonly used for disordered block copolymer melts.[4] In addition, the functional form of this structure factor does not fit the disordered state data well over the entire investigated range of temperatures.

$I(q^*)^{-1}$ is plotted as a function of T^{-1} in Figure 8 for temperatures above T_{ODT}. $I(q^*)^{-1}$ is a nonlinear function of T^{-1} over the entire temperature range studied, which extends 140 °C above T_{ODT}. The curvature indicates deviation from mean-field behavior in this temperature regime and signals that the disordered phase is strongly affected by composition fluctuations.[7,8,17]

In Figure 9, the peak position and width are given. Note that within statistics, no change in q^* is observed at T_{ODT}. This is in spite of a pronounced anomaly in the compressibility at T_{ODT} as measured in a pressure study,[29] implying an intrinsic discontinuity in q^*. The ln q^* versus T curves crosses from one linear portion to another at between 100 and 150 °C. d ln q^*/dT changes from 1.0×10^{-3} to 0.43×10^{-3} K^{-1}. This behavior is similar to what has been seen in a range of other symmetric block copolymers.[8] From the temperature dependence of the unperturbed coil size, $\kappa = \mathrm{d} \ln r_0^2/\mathrm{d}T$, we obtain $\mathrm{d} \ln r_0/\mathrm{d}T = (-0.58 \pm 0.02) \times 10^{-3}$ K^{-1} [30] and $\mathrm{d} \ln r_0/\mathrm{d}T = (0.39 \pm 0.03) \times 10^{-3}$ K^{-1} [31] for PEP and PDMS, respectively. Thus the low-temperature value of d ln q^*/dT far exceeds the bare coil thermal expansivities.

The correlation length in the PEP−PDMS-6 sample is shown in the upper panel of Figure 9 in the form $2\pi/\xi$ in order to make comparison between correlation lengths

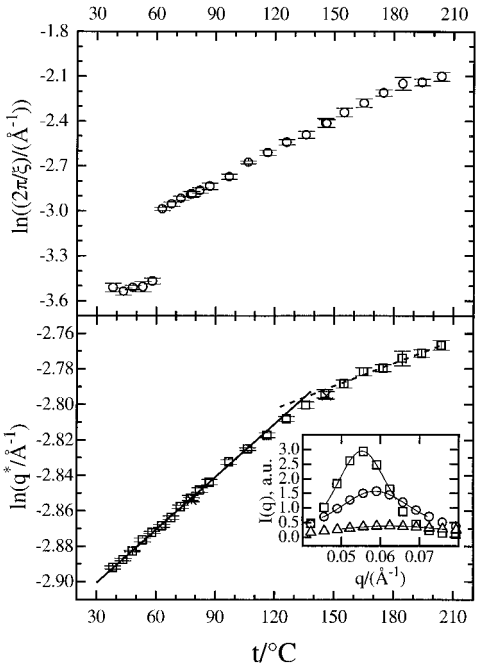

Figure 9. SANS data for sample PEP−PDMS-6 plotted versus temperature. The peaks were fit with a smeared Lorentzian function to obtain peak position q^* and peak width as expressed by the correlation length ξ. Lower: $\ln(q^*)$, increasing temperature (□); decreasing temperature (×). The solid line is least squares fit to the points where $35 < t/°C < 110$ and has the slope $((1.00 \pm 0.01) \times 10^{-3})$ °C^{-1}. The dotted line is least squares fit to the points where $150 < t/°C$ and has the slope $((4.3 \pm 0.6) \times 10^{-4})$ °C^{-1}. Upper: $\ln(2\pi/\xi)$. The inset shows the fit to the SANS data at selected temperatures: 45 °C (□), 97 °C (○), 200 °C (△).

and lamellar spacing easier. At T_{ODT}, ξ decreases discontinuously. It is noteworthy that the correlation length in the ordered state is only approximately two periods of the lamellar structure. This is consistent with the very weak higher order reflection obtained from the ordered state.

In block copolymer melts with higher molar mass, e.g., poly(ethylenepropylene)−poly(ethylethylene) (PEP−PEE),[8,16,17,21] fluctuations above the ODT give rise to relaxation processes characterized by relaxation rates that have a different temperature dependence than the terminal relaxation of the single chain. The relaxation of the fluctuations should also influence the temperature dependence of the viscosity, $\eta = \lim_{\omega \to 0} G''(\omega)/\omega$. In fact, from this relation and from the viscosity of PEP−PDMS-6 just above T_{ODT} (1 Pas), one can estimate the frequency at which sample PEP−PDMS-6 should show the effects of the fluctuation, similar to the high molar mass block copolymers. The loss modulus associated with the process is 2 orders of magnitude lower than the plateau modulus of the block copolymers. Such a modulus would be reached in PEP−PDMS-6 at frequencies of a few krad/s. This frequency domain is experimentally inaccessible on our rheometers. We attempted to access the fluctuation relaxation rate using steady shear in a Couette geometry[32] with shear rates up to $\dot{\gamma} = 10^4$ s^{-1}. SANS measurements conducted close to but above T_{ODT} did not reveal any evidence of shear-induced ordering of the sample.

In a simple polymeric fluid, the temperature dependence of the zero-shear viscosity, η_0, is dominated by the temperature dependence of the longest relaxation time in the system as described by the WLF equation,[33] $\log a_T = -c_1^0(T - T_0)/(c_2^0 + T - T_0)$, where the constants

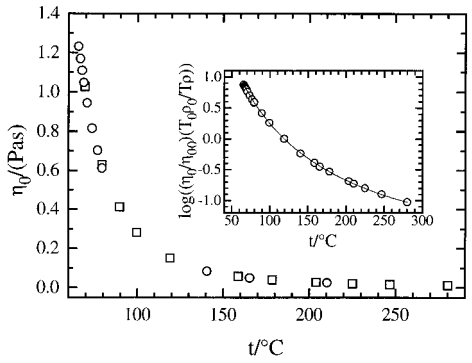

Figure 10. Viscosity of sample PEP−PDMS-6 as a function of temperature. Data were taken while heating (□) and cooling (○). In the inset, the viscosity data are normalized to represent WLF shift factors. The dotted line is a fit to the WLF equation $\log a_T = -c_1^0(T - T_0)/(c_2^0 + T - T_0)$ ($c_1^0 = 2.17$, $c_2^0 = 187.4$ °C, and $T_0 = 119.1$ °C). η_0, and ρ are the viscosity and density, respectively. The subscript zero refers to the reference temperature T_0.

c_1^0 and c_2^0 are characteristic (and known) for a range of polymers. The shift factor, a_T, obeys the relation $a_T = (\eta_0/\eta_{00})(T\rho)/(T_0\rho_0)$, where the second subscript 0 refers to the reference temperature. An eventual contribution of fluctuations to the dynamical mechanical properties of sample PEP−PDMS-6 is therefore expected to be visible as a modification to the WLF behavior close to the ODT. In Figure 10, the viscosity in the linear regime of sample PEP−PDMS-6 is plotted as a function of temperature. A fit of the WLF equation to the data yields the WLF parameters $c_1^0 = 2.25$ and $c_2^0 = 160.8$ °C. The WLF parameters of pure PEP[16] recalculated to 119.1 °C as reference temperature are $c_1^0 = 4.36$ and $c_2^0 = 257.2$ °C. For PDMS $c_1^0 = 1.36$ and $c_2^0 = 311$ °C.[33] Comparing WLF parameters is conveniently done through the Vogel temperature, T_∞, at which the viscosity diverges, assuming that the WLF equation is valid in this limit. This leads to $T_{\infty,PEP-PDMS-6} = -41.7$ °C, $T_{\infty,PEP} = -138.1$ °C, and $T_{\infty,PDMS} = -192$ °C. The $T_{\infty,PEP-PDMS-6}$ is much larger than one should expect from the values for the pure polymers. It can thus be concluded that the segregation phenomena that lead to ordering of sample PEP−PDMS-6 at $T_{ODT} = 64$ °C substantially influence the viscosity at temperatures above T_{ODT}.

4. Discussion

In this paper, we have examined the phase behavior of representative samples from two new diblock copolymer systems. Both of these systems have strong incompatibility between the two types of monomers, *i.e.*, a large χ parameter. One of the issues that has motivated this study is the question of how short a diblock copolymer can be and still behave "polymeric-like". In an earlier publication,[2] we presented a series of block copolymer systems with progressively shorter chains in which PI−PS represented the short-chain limit. The phase behavior of the PI−PS system, even though distinct in the detail, is a natural progression of the behavior found in longer chain block copolymers. We have suggested the following basis for comparing the characteristic chain lengths, N_c and $\bar{N}_c$, for different block copolymer systems:[2] the characteristic values of N and $\bar{N}$ for a symmetric, *i.e.*, $f = 0.5$, block copolymer at which $T_{ODT} = 150$ °C.[8] The N values are based on a common $v = 118$ Å^3 segment volume. For PI−PS $N_{c,PI-PS} = 2.8 \times 10^2$ and $\bar{N}_{c,PI-PS} = 1.1 \times 10^3$. It is not

possible from the data given in the present paper to accurately determine both $\bar{N}_{c,PI-PDMS}$ and $\bar{N}_{c,PEP-PDMS}$ because the temperature dependence of the χ parameter for the two systems is not known. From the characteristic ratio of PDMS, $C_{\infty,PDMS} = 6.54$[20] or $C_{\infty,PDMS} = 7.0$,[34] and κ_{PDMS}, the statistical segment length of PDMS can be estimated to $b_{PDMS} = 4.65 \exp(0.35 \times 10^{-3}(T/K))$. If $\chi \sim A/T$ is assumed for both systems, one can estimate $\bar{N}_{c,PI-PDMS} = 1.5 \times 10^2$, $\bar{N}_{c,PI-PDMS} = 3.9 \times 10^2$, $\bar{N}_{c,PEP-PDMS} = 1.3 \times 10^2$, and $\bar{N}_{c,PEP-PDMS} = 4.6 \times 10^2$. Thus the PI−PDMS and PEP−PDMS systems represent a reduction in chain length of a factor of approximately 3 compared to the PI−PS system.

The $f = 0.65$ sample PI−PDMS-7 exhibits an unprecedented wide range of temperature over which the bicontinuous $Ia\bar{3}d$ phase is stable. In sample PEP−PDMS-7, a set of phase transitions between various ordered states is observed. The trends seen in the longer chain system are thus preserved. Going to shorter chains appears to increase the stability window of the bicontinuous cubic phase. Thus the chain length in the PI−PDMS and PEP−PDMS systems is not short enough to observe deviation from polymer-like behavior.

The increase in T_{ODT} upon saturation of the PI−PDMS sample is particularly interesting. One can estimate the χ parameter from solubility parameter considerations: $\chi = V_0(\delta_1 - \delta_2)^2 R^{-1} T^{-1}$, where V_0 is a reference volume and δ_i is the solubility parameter of component i. The solubility parameter approach is expected to work fairly well for the nonpolar PDMS-containing block copolymers, which are dominated by van der Waals interactions. However, both experimentally and by group contribution methods the δ values fall in a relatively wide range.[35,36] Experimental δ values for PI and PDMS are $16.2 < \delta_{PI} \times 10^3$ Pa$^{-1/2}$ < 20.5 and $14.9 < \delta_{PDMS} \times 10^3$ Pa$^{-1/2}$ < 15.6, respectively, while no data are available for PEP. Fedor's group contribution method[35] indicates $\delta_{PDMS} \simeq 15$ and $\delta_{PEP} < \delta_{PI}$. Other group contribution methods also indicate $\delta_{PEP} < \delta_{PI}$; however, the magnitude of the difference is not consistent. The difference $\delta_{PEP} - \delta_{PI}$ can be estimated from $\chi = 0.022$ at 150 °C in PEP/PI mixtures[37,38] based on the 118 Å^3 reference volume to be 1.0×10^3 Pa$^{1/2}$. Furthermore, the lower experimental δ values appear to be most reliable,[35] and the following values are used to estimate χ parameters: $\delta_{PDMS} = 15.0 \times 10^3$ Pa$^{1/2}$, $\delta_{PEP} = 15.8 \times 10^3$ Pa$^{1/2}$, $\delta_{PI} = 16.6 \times 10^3$ Pa$^{1/2}$. At 150 °C, $\chi_{PI-PDMS} = 0.05$ and $\chi_{PEP-PDMS} = 0.013$. From these values $N_{ODT,PI-PMDS} = 3 \times 10^2$ and $N_{ODT,PEP-PMDS} = 1 \times 10^3$.[8] Thus the solubility parameter consideration predicts a decrease in T_{ODT} upon saturation of PI−PDMS. However, this effect appears to be more than balanced by an increase in conformational asymmetry; $\epsilon_{PI-PDMS} = 1.3$ and $\epsilon_{PEP-PDMS} = 1.5$ at 150 °C. Note also that the $N_{ODT,PMDS}$ estimate is in reasonable agreement with experiment (within a factor of 2.5) whereas the $N_{ODT,PEP-PMDS}$ estimate is off by a factor of 8. A similar effect was found in earlier work between PI−PS and PEP−PVCH[39,40] (PVCH is poly(vinylcyclohexane))diblock copolymers and between PE−PEP and PEP−PEE[2] (PE is polyethylene, and PEE is poly(ethylethylene)). A change in ϵ from 1.5 to 1.7 between PE−PEP and PEP−PEE leads to a twofold decrease in N_{ODT}. Considering the minimal expected change in solubility parameter between PE and PEE, the effect of changing ϵ is of similar magnitude between the PE−PEP/PEP−PEE system and the PI−PDMS/PEP−PDMS system. The modest increase in T_{ODT} observed upon partial saturation of a PS−1,2PB (1,2PB is 1,2-polybutadiene) diblock copolymer to yield a PS−PEE[41] diblock copolymer is of a different nature. In this system, the partial saturation leads to an increase in the solubility parameter difference and a decrease in ϵ.

The effect of conformational asymmetry has been treated theoretically in the athermal limit recently.[1,42] The changes in ϵ are predicted to produce an excess entropy of mixing term, χ_ϵ, which is an increasing function of ϵ and which is additive to other contributions to χ. Thus, in the framework of this mean-field treatment, the ϵ-modification of χ is predicted to decrease on a relative basis when other χ contributions increase. The apparent increase in χ observed in the block copolymers investigated in the present work on increase of ϵ is qualitatively, but not quantitatively, consistent with this prediction. The influence of conformational asymmetry on the χ parameter has also been treated recently by Schweizer and Singh[43] in the context of the polymer reference interaction site model (PRISM). In this theory, the ϵ modification of χ is not additive to other contributions, and thus general qualitative prediction for the influence of ϵ on χ cannot be made. In the athermal limit, the PRISM predicts that χ increases with ϵ. However, the PRISM result also predicts that the athermal entropic modification of χ is negligible compared to enthalpic χ contributions relevant for any homogeneous system.

In earlier work on hydrocarbon-based block copolymers, the temperature, T_x, in the disordered phase where[8] $I(q^*)^{-1}$ versus T^{-1} deviates from linearity was used to identify the crossover from the composition fluctuation regime to mean-field behavior. The width of the fluctuation regime $(\chi N)_x - (\chi N)_{ODT}$ is expected to scale as $\bar{N}^{-1/3}$. As the block copolymers studied in the present work have smaller N, the fluctuation regime is expected to be wider. A proper comparison requires knowledge of $\chi(T)$, which is not available. However, for $\chi(T) = A/T + B$, $\Delta(1/T) = T_{ODT}^{-1} - T_x^{-1}$ will scale as $(NA)^{-1}\bar{N}^{-1/3}$. As NA is approximately constant for block copolymers close to the ODT, $T_x - T_{ODT}$ is expected to increase for $\bar{N}$ decreasing. For the hydrocarbon-based block copolymers, $T_x - T_{ODT}$ ranges between 10 and 75 °C. In PEP−PDMS-6, $I(q^*)^{-1}$ versus T^{-1} is nonlinear throughout the studied temperature range. Thus $T_x - T_{ODT} > 140$ °C. The behavior of the $N \simeq 10^2$ PEP−PDMS-6 sample in the disordered state is as such qualitatively consistent with the fluctuation picture[7] and thus the PEP−PDMS are also polymeric-like with respect to fluctuation behavior in the disordered state. However, the measured magnitude of q^* at the ODT (0.057 Å^{-1}) is not captured. Neglecting molar mass distribution corrections, the mean-field prediction is $q^* = 0.088$ Å^{-1}.[4,44] In the fluctuation theory this number is expected to decrease by 15%.[45]

In higher molar mass diblock copolymers, a fluctuation-mediated mechanical relaxation occurs at frequencies $O(100)$ times lower than the terminal relaxation.[16] The failure to observe shear-induced ordering of the PEP−PDMS-6 sample in the disordered state at $\gamma = 10^4$ s^{-1} is an indication that a similar relaxation cannot be observed around $\omega = 2000$ rad/s at 65 °C. However, the temperature dependence of the viscosity of sample PEP−PDMS-6 clearly indicates a strong contribution to the viscosity from disordered state composition fluctuations. We speculate that the reason for this apparent inconsistency is that the relaxation time of the fluctuations is shifted to times comparable to the

terminal relaxation due to lack of entanglements. In a recent publication on PI−PS diblock copolymers,[46] the weak rheological signal from composition fluctuation in dynamical mechanical spectroscopy is interpreted as absence of composition fluctuations. We believe this interpretation is not warranted.[6]

The disordering of sample PEP−PDMS-7 from the bicontinuous $Ia\bar{3}d$ phase was studied by both rheology and SANS. The measured T_{ODT} is different by close to 10 °C. We note that T_{ODT}'s measured by SANS and rheology usually agree within 1 or 2 °C.[16,21] The value measured by rheology is also only reproducible within a few degrees. At present, we believe the phenomenon is due to a complex temperature and frequency dependence of the dynamical mechanical moduli of the bicontinuous $Ia\bar{3}d$ phase close to the ODT, which is addressed in detail in a separate publication.[18] We also note that the local structure of a fluctuation is body-centered-cubic-like and thus no symmetry chance needs to occurs at T_{ODT} in this case.[47]

5. Conclusions

Transitions between LAM and DIS and $Ia\bar{3}d$ and DIS have been identified in both PI−PDMS and PEP−PDMS block copolymers. These block copolymers represent model block copolymers of molar mass 10^4 g/mol or less. Their phase behavior and the existence of a large fluctuation regime in the disordered state allow us to conclude that these materials have properties that represent a natural progression of phenomena observed in higher molar mass systems. Thus a 6000 g/mol diblock copolymer still behaves very much like high molar mass polymer analogues.

Acknowledgment. This research was supported by the The Engineering Science Centre on Material Structures and Material Models, a Danish Technical Science Research Council sponsored Engineering Research Center at Risø National Laboratory; the Danish Polymer Center, a Research Center at Risø and at the Danish Technical University sponsored by the Programme for Development of Materials Technology; the U.S. National Science Foundation through Grant NSF/DMR-9405101; and the Center for Interfacial Engineering (CIE), an Engineering Research Center at the University of Minnesota. SAXS beam time was provided by the EPSRC; the assistance of Ernie Komanschek in obtaining the SAXS data is much appreciated. F.S.B. and K.A. also benefited from a NATO travel grant.

References and Notes

(1) Fredrickson, G. H.; Liu, A. J.; Bates, F. S. *Macromolecules* **1994**, *27*, 2503−2511.
(2) Bates, F. S.; Schultz, M. F.; Khandpur, A. K.; Förster, S.; Rosedale, J. H.; Almdal, K.; Mortensen, K. *Faraday Discuss. Chem. Soc.* **1994**, *98*, 7−20.
(3) Bates, F. S.; Schulz, M. F.; Rosedale, J. H.; Almdal, K. *Macromolecules* **1992**, *25*, 5547−5550.
(4) Leibler, L. *Macromolecules* **1980**, *13*, 1602−1617.
(5) Helfand, E.; Wasserman, Z. R. In *Developments in Block Copolymers−1*; Goodman, I., Ed.; Applied Science Publishers: London and New York, 1982; pp 99−125.
(6) Bates, F. S.; Fredrickson, G. H. *Annu. Rev. Phys. Chem.* **1990**, *41*, 525−557.
(7) Fredrickson, G. H.; Helfand, E. *J. Chem. Phys.* **1987**, *87*, 697−705.
(8) Rosedale, J. H.; Bates, F. S.; Almdal, K.; Mortensen, K.; Wignall, G. D. *Macromolecules* **1995**, *28*, 1429−1443.
(9) Bates, F. S.; Rosedale, J. H.; Fredrickson, G. H.; Glinka, C. H. *Phys. Rev. Lett.* **1988**, *61*, 2229−2232.
(10) DuPré, D. B. In *Kirk−Othmer Encyclopedia of Chemical Technology*, 3rd ed.; Wiley: New York, 1981; Vol. 14, pp 395−427.
(11) Hillmyer, M. A.; Bates, F. S.; Almdal, K.; Mortensen, K.; Ryan, A. J.; Fairclough, J. P. A. *Science* **1996**, *271*, 976−978.
(12) Almdal, K., to be published.
(13) Tepe, T.; Schulz, M. F.; Zhao, J.; Tirrell, M.; Bates, F. S.; Almdal, K.; Mortensen, K. *Macromolecules* **1995**, *28*, 3008−3011.
(14) Koppi, K. A.; Tirrell, M.; Bates, F. S.; Almdal, K.; Mortensen, K. *J. Rheol.* **1994**, *38*, 999−1027.
(15) Bras, W.; Derbyshire, G. E.; Devine, A.; Clarke, S.; Cooke, J.; Komanschek, B. U.; Ryan, A. J. *J. Appl. Crystallogr.* **1995**, *28*, 26−32.
(16) Rosedale, J. H.; Bates, F. S. *Macromolecules* **1990**, *23*, 2329−2338.
(17) Bates, F. S.; Rosedale, J. H.; Fredrickson, G. H. *J. Chem. Phys.* **1990**, *92*, 6255−6270.
(18) Kossuth, M. B.; Hillmyer, M.; Almdal, K.; Bates, F. S., to be published.
(19) Graessley, W. W.; Edwards, S. F. *Polymer* **1981**, *22*, 1329−1334.
(20) Fetters, L. J.; Lohse, D. J.; Richter, D.; Witten, T. A.; Zirkel, A. *Macromolecules* **1994**, *27*, 4639−4647.
(21) Almdal, K.; Bates, F. S.; Mortensen, K. *J. Chem. Phys.* **1992**, *96*, 9122−9132.
(22) Almdal, K.; Koppi, K. A.; Bates, F. S. *Macromolecules* **1993**, *26*, 4058−4060.
(23) Balsara, N. P.; Hammouda, B. *Phys. Rev. Lett.* **1994**, *72*, 360−363.
(24) Hamley, I. W.; Gehlsen, M. D.; Khandpur, A. K.; Koppi, K. A.; Rosedale, J. H.; Schultz, M. F.; Bates, F. S.; Almdal, K.; Mortensen, K. *J. Phys. II Fr.* **1994**, *4*, 2161−2186.
(25) Hajduk, D. M., manuscript in preparation.
(26) Schultz, M. F.; Bates, F. S.; Almdal, K.; Mortensen, K. *Phys. Rev. Lett.* **1994**, *73*, 86−89.
(27) Hadjuk, D. A.; Harper, P. E.; Gruner, S. M.; Honeker, C. C.; Thomas, E. L.; Fetters, L. J. *Macromolecules* **1995**, *28*, 2570−2573.
(28) Pedersen, J. S.; Posselt, D.; Mortensen, K. *J. Appl. Crystallogr.* **1990**, *23*, 321−333.
(29) Schwahn, D.; Frielinghaus, H.; Mortensen, K.; Almdal, K. *Phys. Rev. Lett.*, submitted.
(30) Zirkel, A.; Richter, D.; Pyckhout-Hintzen, W.; Fetters, L. J. *Macromolecules* **1992**, *25*, 954−960.
(31) Mark, J. E.; Flory, P. J. *J. Am. Chem. Soc.* **1964**, *86*, 138−141.
(32) Mortensen, K.; Almdal, K.; Bates, F. S.; Koppi, K. A.; Tirrell, M.; Nordén, B. *Physica B* **1994**, *213 & 214*, 682−684.
(33) Ferry, J. D. *Viscoelastic Properties of Polymers*; John Wiley & Sons: New York, 1980.
(34) Crescenzi, V.; Flory, P. J. *J. Am. Chem. Soc.* **1964**, *86*, 141−146.
(35) van Krevelen, D. W. *Properties of Polymers: Their Correlation with Chemical Structure; Their Numerical Estimation and Prediction from Additive Group Contributions*. Elsevier: Amsterdam, Oxford, New York, Tokyo, 1990.
(36) Brandrup, J.; Immergut, E. H. *Polymer Handbook*, 3rd ed.; John Wiley & Sons: New York, 1989.
(37) Bates, F. S.; Rosedale, J. H.; Stepanek, P.; Lodge, T. P.; Wiltzius, P.; Fredrickson, G. H.; Hjelm, R. P. *Phys. Rev. Lett.* **1990**, *65*, 1893−1896.
(38) Stepanek, P.; Lodge, T. P.; Kedrowski, C.; Bates, F. S. *J. Chem. Phys.* **1991**, *94*, 8289−8301.
(39) Gehlsen, M. D.; Bates, F. S. *Macromolecules* **1993**, *26*, 4122−4127.
(40) Gehlsen, M. D.; Bates, F. S. *Macromolecules* **1994**, *27*, 3611−3618.
(41) Owens, J. N.; Gancarz, I. S.; Koberstein, J. T.; Russell, T. P. *Macromolecules* **1989**, *22*, 3380−3387.
(42) Bates, F. S.; Fredrickson, G. H. *Macromolecules* **1994**, *27*, 1065−1067.
(43) Schweizer, K. S.; Singh, C. *Macromolecules* **1995**, *28*, 2063−2080.
(44) Vavasour, J. D.; Whitmore, M. D. *Macromolecules* **1992**, *25*, 5477−5486.
(45) Barrat, J. L.; Fredrickson, G. H. *J. Chem. Phys.* **1991**, *95*, 1281−1289.
(46) Han, C. D., Baek, D. M.; Kim, J. K.; Ogawa, T.; Sakamoto, N.; Hashimoto, T. *Macromolecules* **1995**, *28*, 5043−5062.
(47) Almdal, K.; Mortensen, K.; Koppi, K. A.; Tirrell, M.; Bates, F. S. *J. Phys. II* **1996**, *6*, 617−637.

MA960437K